

1 Monitoring Grassland Degradation and Restoration Using a Novel Climate Use 2 Efficiency (NCUE) Index in the Tibetan Plateau, China

3 Ru An ^a, Ce Zhang ^{b, c, *}, Mengqiu Sun ^a, Huilin Wang ^{d, *}, Xiaoji Shen ^{a, e}, Benlin Wang ^a, Fei Xing ^a,
4 Xianglin Huang ^a, Mengyao Fan ^a

5 ^a*School of Hydrology and Water Resources, Hohai University, China*

6 ^b*Lancaster Environment Centre, Lancaster University, UK*

7 ^c*UK Centre for Ecology & Hydrology, Library Avenue, Lancaster, UK*

8 ^d*Department of Geography Information Science, Nanjing University, China*

9 ^e*Department of Civil Engineering, Monash University, Australia*

10 * Corresponding author.

11 E-mail addresses: c.zhang9@lancaster.ac.uk (C. Zhang); huilin_wang@163.com (H.L. Wang)

12
13 **Abstract**—Grassland degradation is one of the most pressing challenges in natural environment and
14 anthropogenic society. However, there is yet no effective approach for monitoring the spatio-temporal pattern of
15 large-scale grassland degradation. In particular, the research on grassland changes in the harsh natural
16 environment such as the Qinghai-Tibet Plateau is still in its infancy due to complexity, and it is extremely
17 difficult for humans to reach these remote areas. The annual changes in the grassland biomass might be the
18 results of climate fluctuations or grassland degradation. To test the hypothesis, the impact of inter-annual
19 climate fluctuations needs to be considered when monitoring the grassland degradation based on spatio-temporal
20 change of grassland biomass. In this paper, we propose a Novel Climate Use Efficiency index (NCUE) by
21 considering rainfall, temperature, sunlight time, wind speed, surface temperature, accumulated temperature, time
22 lag effect, light, temperature and water suitability and their coordination climatic factors that mainly affect
23 vegetation growth comprehensively, to monitor grassland change suitable for cold and dry climate
24 characteristics of the Qinghai-Tibet Plateau, and to reduce the effect of inter-annual variability of grassland
25 productivity caused by climate fluctuation. As a consequence, grassland degradation monitoring could be more
26 accurate and objective than existing ecological indicators. Our experiments show that the slope of NCUE over
27 31 years from 1982 to 2012 is 0.0028, showing a recovery trend in grassland. Degradation and restoration of
28 grassland exist at the same time, and their proportions are 20.49% and 23.89%, respectively. By comparing with
29 in-situ measurements in 2013 and 2009, 68% consistency was achieved with our prediction, and the 70%
30 consistency is achieved by comparing with the positive and negative change trend of accumulated NDVI during
31 the growing season. Moreover, the comparative analysis of land use/cover changes (LUCC) from 1990 to 2010

32 shows 69% of consistency. The ratio of the area of grassland significantly degradation and recovered predicted
33 by NCUE change trend is 1.41% and 1.43%, respectively. It occupies a very small area of the study area. Yet,
34 that predicted by NDVI change trend is 42.17% and 31.90%, respectively, and about 70% of the area is detected
35 as drastic changes. It shows that NDVI is sensitive to climate fluctuations, while NCUE reduces the impact of
36 climate fluctuations, reflecting change of grassland being affected by human activities and long-term climate
37 change. The novel NCUE has great potential and utility to minify the impact of climate fluctuation and reflect
38 grassland changes over space and time quantitatively. Such ecological index provides a new understanding of
39 spatial and temporal patterns of grassland degradation in the Three River Headwaters Region (TRHR) at the
40 same time.

41 Keywords: Grassland degradation and restoration, RUE, NCUE, IMF, TRHR, Tibetan Plateau.

42 **1. Introduction**

43 Grasslands are one of the most important parts of natural ecosystems. Grassland degradation refers to significant
44 changes in the composition, structure, and function of grassland ecosystems influenced by human activities or
45 climate-related natural factors. Grassland degradation is manifested as the decline of quality in the grassland
46 ecosystem (including vegetation and soil), productivity, economic potential and ecosystem services, the
47 deterioration in ecological environment, and the decrease in biodiversity and landscape complexity, whilst
48 recovery functions are weak or lost completely (Wang, 2004). China is the second-largest steppe country in the
49 world, and natural grassland accounts for 40% of the country's total area of land. In recent decades, China's
50 grasslands have experienced large-scale desertification, degradation, and salinization, which form an important
51 source of sandstorms.

52 Grassland degradation is a major issue related to the sustainable development of the social economy (Li, 1997).
53 At present, the monitoring of grassland degradation mainly includes field observation and inspection methods
54 (Gu et al., 2010; Wang et al., 2004; Xue et al., 2009) and remotely sensed methods (An et al., 2017, 2014; Chen
55 et al., 2010; Gardiner et al., 2016; Li, 1997; Nicholson et al., 1998; Wang et al., 2014; Zhang et al., 2017; Zhao,
56 2012). The former type of methods is accurate, but they are labor-intensive and time-consuming, and subject to
57 local experience and expertise. The indicators of grassland degradation mainly include biological indicators (e.g.
58 vegetation coverage, biomass, dominant species, etc.) and soil traits (Yan, 2008). Soil traits are extremely
59 difficult to obtain at regional scales, whereas biological indicators are often used to evaluate large-scale
60 grassland degradation. Remote sensing methods can provide information on the vegetation coverage, biomass,
61 etc. at large regional scales. Therefore, changes in vegetation coverage or biomass information derived from
62 remotely sensed imagery are often used to evaluate grassland changes (An et al., 2017; Bastin et al., 2012; de

63 Jong et al., 2011; Eddy et al., 2017; Fensholt et al., 2012; Geerken and Ilaiwi, 2004; Karnieli et al., 2013; Li et
64 al., 2012; Liu et al., 2008; Meroni et al., 2017; Sandra et al., 2015). With the increasing use of remotely sensed
65 imagery and products such as AVHRR, MODIS and SPOT VEGETATION (de Jong et al., 2011; Li et al.,
66 2020), more attention has been paid to characterize the changes of grassland productivity through trend analysis
67 of long-term sequence vegetation indices (such as the Normalized Difference Vegetation Index (NDVI) as a
68 proxy for the net primary productivity (NPP) or above-ground biomass) (Bai et al., 2008; Fensholt et al., 2012;
69 Shen et al., 2018). However, these methods do not take into account reducing the effects of climate fluctuations
70 on grassland productivity over the years and may not be able to reflect the real grassland condition. In addition
71 to human activity, the vegetation status and growth rates are also dependent on the climatic conditions affected
72 by water availability and thermal conditions. Regional climates have certain fluctuations and periodicity. The
73 periodic climatic factors (such as precipitation, temperature, etc.) will cause "poverty years" and "abundant
74 years" of grassland plant growth across different years. The annual changes in the grassland biomass might be
75 the results of climate fluctuations or grassland degradation. Similarly, the grassland biomass could be used as a
76 proxy indicator to evaluate grassland degradation, and the impact of climate fluctuations need to be considered
77 to better understand grassland changes. Researchers have previously adopted the rainfall use efficiency (RUE)
78 (Brown de Colstoun et al., 1998; Gao et al., 2005; Holm et al., 2003) and energy use efficiency (EUE) to reduce
79 the impacts of climate fluctuations (Bai et al., 2008; Brown de Colstoun et al., 1998; Houerou and Henri N.,
80 1984), with the applications on grassland degradation areas. In addition, there are other methods developed for
81 monitoring grassland degradation by considering climate impacts include LNS (Local NPP Scaling) (An et al.,
82 2017; Prince, 2012; Prince et al., 2009; Wessels et al., 2008), and time-series analysis using nonlinear
83 seasonal-trend analysis (Prince, 2012; Sandra et al., 2015; Shen et al., 2018), the residual trend analysis method
84 derived from the RUE (Burrell et al., 2017; Cai et al., 2015; Evans and Geerken, 2004; Leroux et al., 2017; Li et
85 al., 2012; Wessels et al., 2007; Xu et al., 2010) and the simulation of the potential NPP through global
86 vegetation physiological and biochemical models such as the Lund-Potsdam-Jena dynamic vegetation
87 model(LPJ) (Seaquist et al., 2008; Zika and Erb, 2009).

88 The processes and causes of grassland degradation have received significant attention (Zhang et al., 2017), and
89 the research on grassland degradation is still in its infancy due to the complexity (Yan, 2008). Both equilibrium
90 and non-equilibrium models were adopted to unravel the mechanism of grassland vegetation succession (Vetter,
91 2005). The equilibrium model highlights the importance of biotic feedback such as the density-dependent
92 regulation of livestock populations and the feedback on livestock density with respect to vegetation composition,
93 cover and productivity. In contrast, non-equilibrium rangeland systems are thought to be driven primarily by
94 stochastic abiotic factors, notably, variable rainfall, which results in highly variable and unpredictable primary

95 production. Recent studies suggest that most arid and semi-arid rangeland systems encompass elements of both
96 equilibrium and non-equilibrium at different scales. Therefore, the monitoring of spatial-temporal patterns of
97 large-scale grassland degradation is still lack of an effective and generalized method.

98 This research focuses on the three river headwater region (TRHR), which is the birthplace of three major rivers,
99 the Yangtze, Yellow and Lancang Rivers, is located in the hinterland of the Qinghai-Tibet Plateau. It is an
100 international research hotspot and has a vast area with a harsh natural environment of high altitude, thin air, and
101 a dry and cold climate. This has brought challenges in data acquisition and field-based research, and caused
102 differences in the understanding of degraded grassland areas, spatial distribution characteristics, and
103 degeneration causes in the area (An et al., 2017; Harris, 2010; Liu et al., 2008; Verón et al., 2006; Wu et al.,
104 2014; Zhang et al., 2017; Li et al.,2020).

105 In recent years, researchers have made pioneering explorations on grassland dynamics in the study area.
106 Different methods, data and indicators have been developed and applied for remotely sensed monitoring of
107 grassland changes. For example, grassland change information was derived by comparing multi-period
108 grassland status data based on visual interpretation and human-computer interaction (Liu et al., 2008); Different
109 ecological units or production capacity units were divided for grassland according to natural conditions, and
110 un-degraded reference values was identified at the same unit, and such indicator was adopted to quantify the
111 grassland degradation (Wu et al., 2014; An et al., 2017); DBEST (Detecting Breakpoints and Estimating
112 Segments) was applied for trend analysis of NDVI time series, such that vegetation change was detected and the
113 impact of ecological conservation was demonstrated (Shen et al., 2018); The combination of vegetation
114 coverage and spatial heterogeneity indicators was used to identify grassland conditions and monitor changes in
115 grassland (Li et al., 2020). Vegetation dynamics and its driving factors in the study area from 1982 to 2012 have
116 been explored, where the dominant factors for grassland changes are distinct over different periods (Zhang et al,
117 2016). The major remote sensing data sources used are NOAA / AVHRR-NDVI, MODIS-NDVI, and Landsat
118 series imagery. The indicators used for monitoring involve NDVI, NPP, vegetation coverage, spatial
119 heterogeneity, etc.

120 In this research, we comprehensively considered multiple meteorological factors and constructed a novel
121 ecosystem characteristic index suitable for the climatic characteristics of TRHR to monitor grassland dynamics
122 by combining remote sensing and time-series climate data. The main scientific contribution of this paper are as
123 follows: (1) Propose a Novel Rainfall Use Efficiency index (NCUE) for monitoring grassland dynamic which is
124 suitable for cold and arid climate characteristics of the Qinghai-Tibet Plateau to reduce the effect of inter-annual

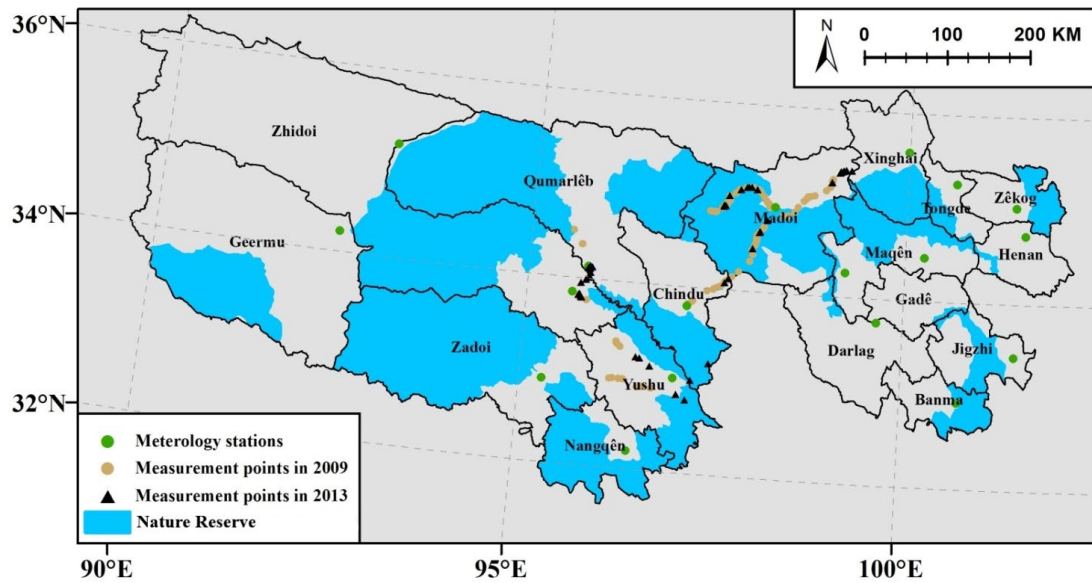
125 variability of grassland productivity caused by climate fluctuation; (2) Construct an Integrated Meteorological
126 Factor (IMF) based on the analysis of dominate climatic elements affecting vegetation growth; (3) Reveal the
127 spatial temporal characteristics of grassland change from 1982 to 2012 in the TRHR by trend analysis of NCUE
128 time series. A new understanding of the grassland dynamics in the study area was gained. In addition to the
129 rainfall factor that affects the growth of vegetation derived in RUE, our proposed novel NCUE also considers
130 the effects of temperature, land surface temperature, wind speed, sunlight, as well as time lag to build an
131 integrated meteorological index IMF. Such NCUE is suitable for the “cold and dry” characteristics of the study
132 area and has the ability to reduce the impact of integrated climate fluctuations and detect grassland degradation
133 objectively.

134 **2. Study area and data source**

135 *2.1 Study area*

136 The TRHR is located in the southern part of Qinghai Province at 31°39' to 36°12' north latitude and 89°45'
137 to 102°23' east longitude. The whole area covers approximately 360 000 km², and it includes 16 counties of
138 Yushu, Guoluo, Hainan and Huangnan, and the Tanggula township of Golmud City (Fig. 1). The Tanggula
139 township appears as Geermu in Fig. 1. The elevations range between 2800m and 6564m. The main mountain
140 ranges in TRHR are the East Kunlun Mountains and their branch veins, the Animaqing Mountain, Bayankara
141 Mountain and Tanggula Mountain Range. There are numerous rivers and lakes, and swamps are widely
142 distributed across the area. The vegetation types are predominantly alpine meadows and alpine grasslands. The
143 area has the highest concentration of biodiversity in high-altitude regions in the world. The originality and
144 vulnerability of the vegetation are well documented (Liu et al., 2005). The climate of the TRHR belongs to the
145 Qinghai-Tibet Plateau climate system, and it is a typical continental climate at high altitude (Li et al., 2006).
146 TRHR is characterized by alternating hot and cold seasons, small annual temperature differences, large daily
147 temperature differences, long sunshine duration, and strong radiation, and the distinction among four seasons is
148 not obvious throughout the year.

149 The nature reserves in TRHR are currently the largest in China. The nature reserves are divided into 6 regions
150 and contain 18 protected sub-areas, with a total area of 152000 km², accounting for 42% of the total area of the
151 TRHR. The distributions of the research area, nature reserves, field observation sites and weather stations are
152 shown in Fig. 1.



153
154 Fig.1. Distributions of research areas, nature reserves, filed observation sites and weather stations

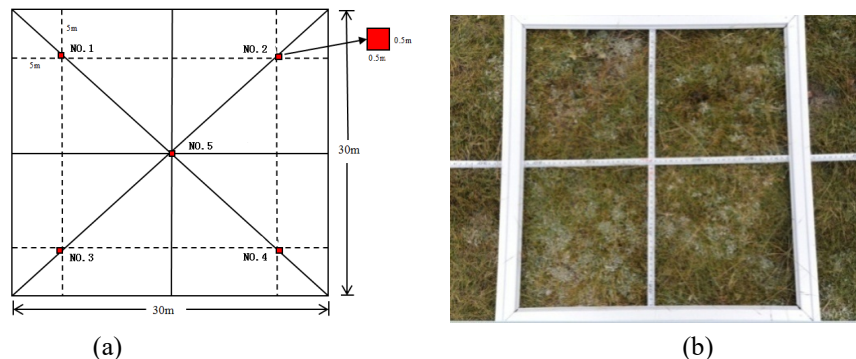
155 2.2. Data Source

156 The NDVI data used in this research are NOAA/AVHRR-NDVI data from 1982 to 2001 and
 157 Terra/MODIS-NDVI (MOD13) data from 2000 to 2012. The AVHRR-NDVI data are from the Pathfinder
 158 AVHRR NDVI, which is freely available from the China Western National Environmental and Ecological
 159 Scientific Data Centre (<http://westdc.westgis.ac.cn>). The dataset has a temporal resolution of 10 days and a
 160 spatial resolution of 8km×8km. The 16-day Terra/MODIS-NDVI data with a spatial resolution of 250 m was
 161 obtained from the NASA (<https://modis.gsfc.nasa.gov/>).

162 The daily meteorological data from 36 weather stations in the study area and its surrounding areas were acquired
 163 from 1982 to 2012. At the same time, a high-precision 0.5° × 0.5° grid data set (V2.0) was used, including daily
 164 rainfall value, monthly value, daily surface temperature, and monthly value of the ground surface in China. The
 165 data was downloaded from China Meteorological Data Service Centre (<http://data.cma.cn>). The China Regional
 166 Surface Meteorological Elements data set (ITPCAS) (He and Yang,2014) and grid data set of CRU TS 3.21 with
 167 spatial resolution of 0.5° × 0.5° were also adopted (Huang et al., 2013).

168 The land use/cover (LULC) data at a scale of 1:100,000 was downloaded from the Chinese Academy of
 169 Sciences Resource and Environmental Science Data Center, covering the temporal range from the 1980s, 1990,
 170 1995, 2000, 2005 and 2010 (<http://www.resdc.cn>). Visual image interpretation was employed to identify LULC
 171 types using the Landsat TM/ETM+ satellite images at the corresponding dates. These LULC data were
 172 classified into six primary types initially, which were cultivated land, woodland, grassland, water bodies,
 173 residential areas and unused areas. Then, twenty-five secondary types were further classified. Cultivated land

174 refers to paddy fields and dry croplands. Woodland refers to woodland, shrubbery, sparse woodland and other
 175 wooded lands. Grassland refers to high-coverage grassland, medium-coverage grassland and low-coverage
 176 grassland. Water bodies include rivers, canals, lakes, reservoirs, pits, glaciers, permanent snow, tidal flats and
 177 beaches. Residential areas refer to residential land in urban, rural, industrial and mining areas. Unused areas
 178 contain sand, Gobi, saline-alkali, marsh, bare land, bare rocky gravel and other unused land types. Bare land in
 179 the unused areas refers to a large area of bare land with almost no grass distributed in it. Bare soil contained in
 180 degraded pastures is not included in the unused areas. Usually, grass and bare soil are mixed in degraded
 181 pastures. The LULC data was used for comparative analysis of the detected grassland change results.
 182 From August 11 to 21 in 2013, a comprehensive field survey and spectral measurements were conducted in the
 183 study area. The route and the selection of the quadrat locations (Fig. 1) were designed based on satellite
 184 imagery, Google Maps, road and river distribution maps, topographic maps, LULC maps and grassland resource
 185 maps. The sampling sites were chosen on both sides of roads where the terrain was flat and open, and the degree
 186 of grassland degradation was relatively uniform. They were sparsely distributed and were at least 2 km apart
 187 from each other. The spectra of various grass species, bare soil, water bodies, and various degrees of degraded
 188 grassland were measured extensively.



189
 190
 191 Fig.2. The sketch of the sampling spots: (a) 30×30 m² large quadrat; (b) 0.5×0.5 m² small quadrat
 192 The sample area is 30×30m². GPS determined the center position of the sample. Using the “X” sampling method
 193 (Fig. 2), five sampling points were placed within each large sample, and a 0.5×0.5 m² sample box was placed at
 194 each sampling point. Expert knowledge was used to visually estimate the vegetation coverage, including the
 195 total coverage and component coverage of various grass species within the 0.5×0.5 m² sample boxes. An error
 196 of less than 5% was achieved when compared with the results identified from photographs taken in the field.
 197 The 30×30 m² large square coverage was obtained based on the average coverage of five small squares. At the
 198 same time, photographs and records at the location of each sample site, along with weather conditions and
 199 geographical features were collected comprehensively (Fig. 3). A total of 56 30×30 m² quadrats were obtained

200 for the delineation of the grassland degradation level. These were used for comparative analysis of the grassland
201 changes derived in the research. Moreover, the administrative boundary vector maps, nature reserve vector map,
202 DEM data with a 100-meter resolution, and a Qinghai Province 1: 1,000,000 grassland type distribution map of
203 the TRHR were used. The DEM data was used for meteorological data interpolation, and the grassland type
204 distribution map was used for extracting grassland information.
205 In August, 2009, a comprehensive field survey was also conducted. Based on the experience of experts, the
206 grassland situation of 70 inspection sites was recorded. This information will also be used for comparative
207 analysis of the results of this article.



208
209 (a) (b)
210 Fig.3. Typical extremely degraded grassland landscape: (a) Iron bar hammer – a typical degraded grass species,
211 at Zarlina Lake; (b) "Black Earth Beach" rodent

212 3. Methods

213 There are six main research steps in this paper, including data collection, data preprocessing, IMF
214 construction, NCUE establishment and grassland changes monitoring, analyzing the spatiotemporal
215 characteristics of grassland changes, and analyzing and discussing the results. Detailed descriptions of the
216 methodology are presented in the following sections.

217 3.1. Data preprocessing

218 3.1.1. Preprocessing remotely sensed data

219 The preprocessing step included projection transformation, monthly maximum NDVI synthesis, and scale
220 transformation. Both NOAA/AVHRR-NDVI and MODIS-NDVI (MOD13) were projected onto the Albers
221 Conical Equal Area. NDVI composites were created using the maximum value composite (MVC) technique
222 (Holben, 1986), using the highest AVHRR-NDVI from daily images over 10-day periods. The MODIS-NDVI
223 from daily images over 16-day periods was selected as the least affected by clouds or the atmosphere.
224 Correlation analysis of the overlapping period of the two different NDVI data in 2000-2001 was carried out, and

225 a linear regression model was fitted to modify the differences of the NDVI between two different sensors (Lu,
226 2011). The estimated NOAA 8km × 8km/AVHRR NDVI was resampled to a 250-m spatial resolution to be
227 consistent with that of MODIS-NDVI. The NDVI values for each month of the growing season were
228 accumulated to obtain the cumulative NDVI (\sum NDVI) in the growing season.

229 After analyzing the meteorological station-measured temperature data, it was found that from May 8 to
230 September 28, the temperature was stable at 0 °C or above during the majority of years, so this period was
231 regarded as the growing season. In this case, the growing season lasts from May to September (Lu, 2011).

232 3.1.2. Spatialization of climatic elements using multiple data sources and multiple methods

233 First, a cumulative treatment was applied to the rainfall at the monthly scale and the scale of growing
234 seasons. Mean values were used for temperature, sunshine duration, wind speed, and surface temperature.
235 Meteorological stations in the TRHR are scarce, especially in the west, which affects the accuracy of
236 interpolation. The spatial resolution of existing grid data is $0.5^{\circ} \times 0.5^{\circ}$ (i.e., an average spatial resolution of
237 49.0 km for longitude and 55.6 km for latitude), which does not match the spatial resolution of MODIS NDVI at
238 250 meters. According to Gao et al. (2014), we used the data of the grid cell center (derived from grid data sets)
239 and weather stations to perform further interpolation to obtain grid data with a spatial resolution of 250 meters.
240 GRADS 2.0 was used to generate the corresponding grid center point data. These grid center points were used
241 as supplemental sites, and then ArcGIS Geostatistics software was used for interpolation. For many spatial
242 interpolation methods for meteorological data, there is no optimal interpolation method suitable for all
243 meteorological elements. After analysis and comparison, rainfall and sunshine hours were rasterized using
244 Geostatistics Ordinary Kriging (OK), and cross-validation showed that the accuracy was over 90%. The
245 temperature and land surface temperature were rasterized using multiple regressions and residual OK methods
246 with an accuracy of 90%. The wind speed was rasterized using topographic factor correction (Fu, 1983; Lu et
247 al., 2009), and the accuracy was over 85%. The interpolation results could meet the research requirements of
248 this paper.

249 3.2 *Integrated meteorological factor (IMF) construction*

250 The growth of grassland vegetation is mainly affected by the climate, soil, grass species characteristics itself,
251 and human activities. For a certain region, changes in the soil properties and grass species composition are
252 relatively stable over a specific time scale, while the climatic factors fluctuate significantly each year, which
253 may lead to annual changes in grassland vegetation. Sunlight, temperature and precipitation are the basic

254 climatic factors affecting vegetation growth (Gu et al., 2010; Lu, 2011; Qian et al., 2010, 2007; Yu, 2013). The
255 TRHR has cold climatic conditions and the existence of frozen soil has great impacts on the grassland
256 vegetation growth (Xue et al., 2009). The surface temperature is an important factor affecting the frozen soil.
257 Precipitation is also a limiting factor of vegetation growth in the study area (Wang et al., 2014). In addition, the
258 strong wind speed and its variation in the region will affect the regional evaporation and soil moisture. As a
259 consequence, vegetation growth is also influenced (Gardiner et al., 2016; Zhao, 2012). The response of
260 grassland vegetation to the climate has lag effects (An et al., 2014; Zhang et al., 2017), and different regions and
261 vegetation types have different responses to the climate (Chen et al., 2010). Therefore, the main climatic factors
262 were chosen as the temperature, precipitation, sunshine, surface temperature, wind speed, and lag effects.
263 Using data from thirteen meteorological sites and the Pearson correlation analysis, the relationship between
264 \sum NDVI and each climatic factor was established for each year. Then, take the 31-year average as the multi-year
265 average correlation coefficient. It was found that \sum NDVI has a good correlation with each climatic factor, and
266 all passed the $p < 0.01$ significance test. Five climatic factors in the growing season were chosen as the main
267 climate impact factors.

268 The time lag responses of \sum NDVI to the five types of climatic factors in the region are different. For the
269 temperature, the correlation between \sum NDVI and the temperature in April of each year is the highest, of which
270 the lag period of the temperature response maybe one month. For the wind speed, the highest correlation appears
271 in March, and the lag period maybe approximately two months. For the surface temperature, the highest
272 correlation appears in February, and the lag period maybe three months. For precipitation and sunshine hours,
273 the correlations reach the maximum during the growing season, and the lag period maybe less than one month.
274 Thus, the three factors of the average temperature in April, the average wind speed in March, and the average
275 surface temperature in February were selected as the major time-delay factors. The correlation analysis of the
276 cumulative NDVI in the growing season and the effects of the time lag of various climatic factors are listed in
277 Table 1. An annual accumulated temperature of greater than 0 °C is used to characterize the heat demand for
278 vegetation growth and development (He and Yang, 2014), which was also selected as one of the major climate
279 impact factors.

280 In addition, evaluations of the local appropriate degree of rainfall, temperature and sunshine for grassland
281 vegetation growth were conducted. All the suitability values of every 10 days during the growing season were
282 derived by adding them together. They were named as the rainfall condition index, temperature condition index
283 and sunshine condition index, respectively, and chosen as three key indices.

284 Taking the water conditions of a particular 10 days as an example, the suitability value is computed as follows
 285 (Qian et al., 2007):

286 When the precipitation reaches the perennial average of 10 days, this indicates that the water supply meets the
 287 normal standard for grassland vegetation adaptation. At this time, the water condition index is assumed to be 1.
 288 Precipitation of less than 50% during the normal period is regarded as the limit of the lack of precipitation
 289 (drought). The rainfall suitability model for 10 days is derived as:

$$290 \quad I_p = \begin{cases} 1 & p \geq \bar{p} \\ \frac{1}{1 + ((\bar{p} - p) / p_m)^2} & 0 \leq p < \bar{p} \end{cases} \quad (1)$$

$$291 \quad p_m = 0.5\bar{p} \quad (2)$$

292 Where I_p is the rainfall suitability value for 10 days. P is the precipitation during this 10-days valuation period.

293 \bar{p} is the perennial average value during the evaluation period. p_m is the lower bound of precipitation. For the
 294 calculations of the temperature and sunshine suitability values, please refer to Qian et al. (2007). Precipitation,
 295 temperature and sunshine are mutually restricted and interacting with each other. If these three elements are
 296 matched and coordinated, the overall meteorological conditions will be conducive to the growth of grassland
 297 vegetation, but if anyone element deviates, it will limit the play of the other elements. According to this
 298 principle, the light, temperature and water matching index (STPC) (Huang et al., 2013; Lu, 2011; Qian et al.,
 299 2007; Yang, 2012) was constructed and selected. The index takes the minimum of the three conditional indices
 300 of the growing season, which is also referred to as the principle of minimum restriction (Qian et al., 2007).

301 Based on these selected climate factors, an integrated meteorological factor (IMF) index is established to
 302 capture the multiple linear relationships. The IMF is expressed as:

$$303 \quad IMF = a_1X_1 + a_2X_2 + a_3X_3 + \dots + a_nX_n \quad (3)$$

304 Where $X_1, X_2, X_3 \dots X_n$ are meteorological factors that affect the vegetation NDVI, $a_1, a_2, a_3, \dots a_n$ are the weight
 305 coefficients of each factor, and n is the number of selected meteorological factors. In this paper, n is 13. The
 306 IMF characterizes both climatic contributions to the NDVI, and also reflects the comprehensive meteorological
 307 conditions affecting the vegetation growth.

308 Using the yearly \sum NDVI as the dependent variable and corresponding climatic factors as independent
 309 variables, then, we can establish an equation set of 31 equations and a linear equation was fit on a per-pixel level
 310 by regression analysis using ordinary least-squares or partial-least-squares and the contribution weight of each

311 climatic factor would be achieved as a pixel-wise IMF estimation. The specific climate factor values of a certain
 312 year were brought into eq. 3, and integrated meteorological factor can be obtained for each pixel of each year.
 313 Table 1 Correlation between the cumulative NDVI during the growing season and the climatic factors of each month before
 314 the growing season

	Average temperature	Cumulative rainfall	Average sunshine hours	Average wind speed	Average surface temperature
January	0.490**	0.755**	-0.557*	-0.780**	0.514**
February	0.518**	0.838**	-0.575*	-0.781**	0.536**
March	0.524**	0.869**	-0.641*	-0.810**	0.388**
April	0.530**	0.860**	-0.717**	-0.806**	0.429**
Growing season	0.418**	0.889**	-0.824**	-0.788**	0.511**

315 (*: p<0.01; **: p<0.001)

316 3.3 The grassland ecosystem characteristics index (NCUE) and grassland changes monitoring

317 3.3.1. Establishing the NCUE

318 The rainfall use efficiency (RUE) is defined as the ratio between the annual aboveground primary
 319 production and the annual precipitation. It can be calculated from remotely sensed biomass (such as the NDVI)
 320 and precipitation data. The TRHR has the characteristics of "cold and dry", and precipitation is not the single
 321 climatic factor that affects the growth of grassland vegetation. Thermal conditions play an important role in the
 322 growth of grassland vegetation. Similar to the RUE, the IMF, which is composed of multiple climatic factors
 323 affecting vegetation growth, was introduced into NCUE model, and a grassland ecosystem characteristic index
 324 (NCUE) suitable for the climatic characteristics of the study area was established:

$$325 \quad NCUE = \frac{\sum NDVI}{IMF} \quad (4)$$

326 Where NCUE is the grassland ecosystem characteristics index, $\sum NDVI$ is the NDVI accumulation of the
 327 growing season, and IMF is the integrated meteorological factor. If the NCUE declines over time, the conditions
 328 of the grassland may become worse. If the NCUE is on the rise over time, this means that the grasslands might
 329 be improved. If the trend of the NCUE is unchanged, this indicates that the grassland status may remain
 330 unchanged. In this study, $\sum NDVI$ was chosen as the proxy indicator of the annual vegetation biomass of
 331 grassland (Stow et al., 2004; Sun, 2015).

332 3.3.2. Trend analysis of the NCUE to Monitor Grassland Changes

333 A trend analysis of NCUE time-series data from 1982 to 2012 was performed to determine the changes of
 334 grassland at the pixel level. This established a linear regression over time. The slope and correlation coefficient
 335 of the regression equation were calculated, and the correlation coefficient was tested statistically at a 95%
 336 confidence interval. A negative slope value defines degradation and a positive value reflects recovery. The
 337 greater the absolute value of the slope, the higher the degree of grassland degradation or restoration. The
 338 significance of time-series trends is used to characterize changes in grasslands, such as significant degradation,
 339 degradation, recovery and significant recovery. Significant degradation describes an area that has a negative
 340 slope and passes the 95% confidence interval, while degradation (but not significant) refers to the areas that
 341 have a negative slope but do not pass the significant test. Recovery (but not significant) refers to areas with
 342 positive slopes but do not pass the significant test. Significant recovery refers to areas with significantly positive
 343 slopes at a 95% confidence interval. Unchanged refers to areas with a slope of $-0.0017 \sim 0.0013$ (these
 344 thresholds were determined based on the field observation and LULC data).

345 *3.4 Comparing and analyzing the rangeland changes*

346 The field observed data acquired in 2013 and 2009, land use/cover change maps and the change trend of
 347 accumulated NDVI in the growing season were used to compare and analyze the monitoring results of grassland
 348 degeneration. According to Pan (2007), a two-steps cluster is employed based on the analysis of grassland
 349 conditions, division standard and the study area situation. The input data is the native plant species, poisonous
 350 weeds, and bare soil component with coverage of sample plots. The grading standards of the grassland status
 351 were obtained thereafter. The grassland status was classified into five categories of non-degradation, mild
 352 degradation, moderate degradation, severe degradation and extreme degradation (Pan, 2007; Yu et al., 2012)
 353 (Table 2). The changing trend of the NCUE from 1982 to 2012 is different from the grassland degradation
 354 situation according to their definitions. Although the former is the changing trend and the latter is the change
 355 outcome, these two might have some connections.

356 Table 2 Degradation degree judgment matrix of alpine meadow grassland

Degradation level	Native plant species ratio (%)	Poisonous weeds ratio (%)	Bare soil ratio (%)
Non-degradation	≥ 72	≤ 15	≤ 10
Mild degradation	55-72	15-35	10-25
Moderate degradation	35-55	35-50	25-50
Severe degradation	20-35	50-75	45-80

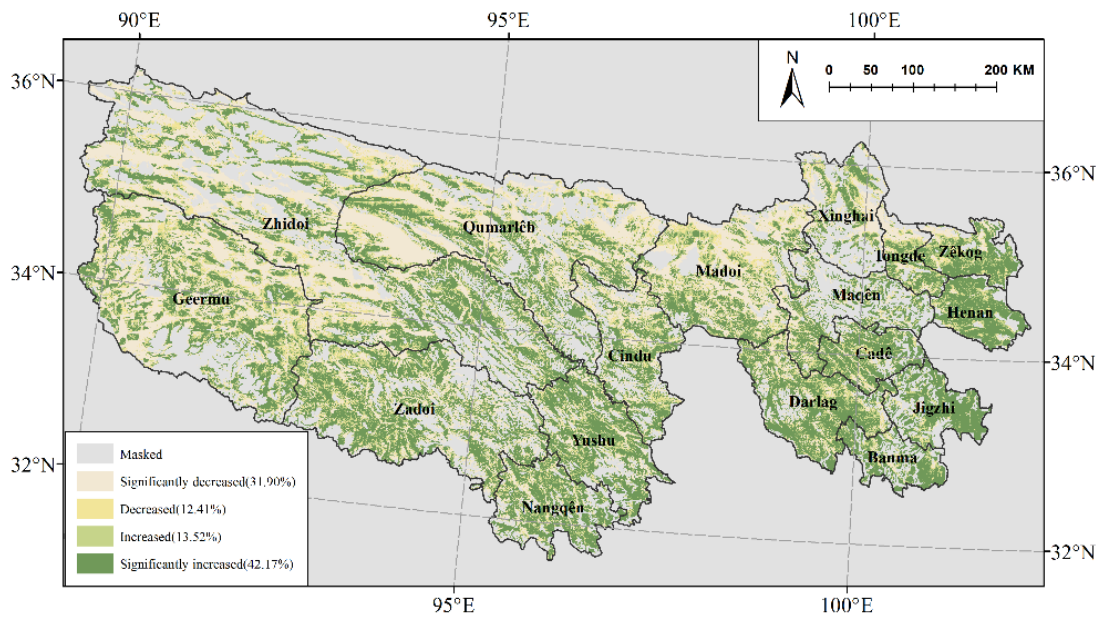
357

358 4 Experimental results and analysis

359 4.1 Changing trend of accumulated NDVI during the growing season, the IMF and NCUE

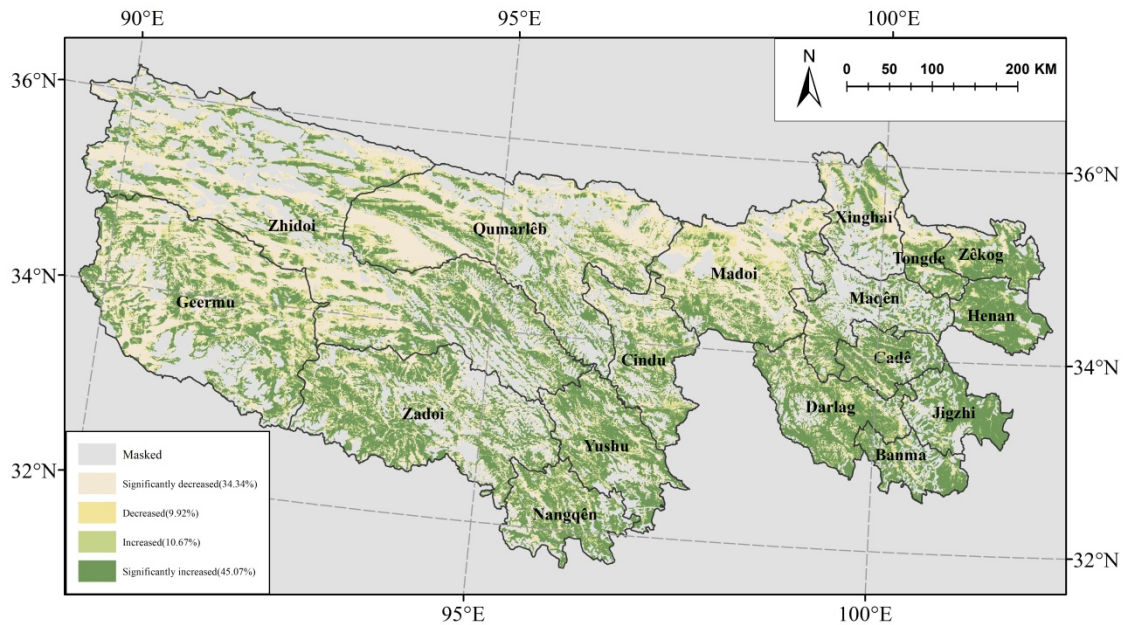
360 Changing trend from 1982 to 2012 for accumulated NDVI during the growing season is shown in Fig. 4. It
 361 indicates that from 1982 to 2012, the NDVI in TRHR showing an overall increase trend. The percentage of
 362 significantly increased NDVI is 42.17%, which cover the largest area of the TRHR, while the percentage of
 363 insignificantly increased is 13.52%; the percentage of significantly decreased NDVI from 1982 to 2012 is
 364 31.90%, cover the secondary largest area of the TRHR, and the percentage of insignificantly decreased NDVI is
 365 12.41%.

366 The significantly increased NDVI mostly distributed in southeast and south center of the TRHR, such as Zêkog,
 367 Henan, Jigzhi, Banma, Darlag, south and center part of Xinghai, Yushu, Nangqên, Zadoi, Cindu and the south
 368 part of the Zhidoi, while the insignificantly increased NDVI mostly distributed in west part of the TRHR, such
 369 as Geermu and the north part of Zhidoi. The significantly decreased NDVI were mostly distributed in the north
 370 and center part of the TRHR, such as the most part of Madoi, east and west part of Qumarlêb that adjacent to
 371 Madoi and Zhidoi, center and north part of Zhidoi, east and northeast part of Geermu that adjacent to Zhidoi.



372

373 Fig.4. Change trend from 1982 to 2012 for accumulated NDVI during the growing season



374

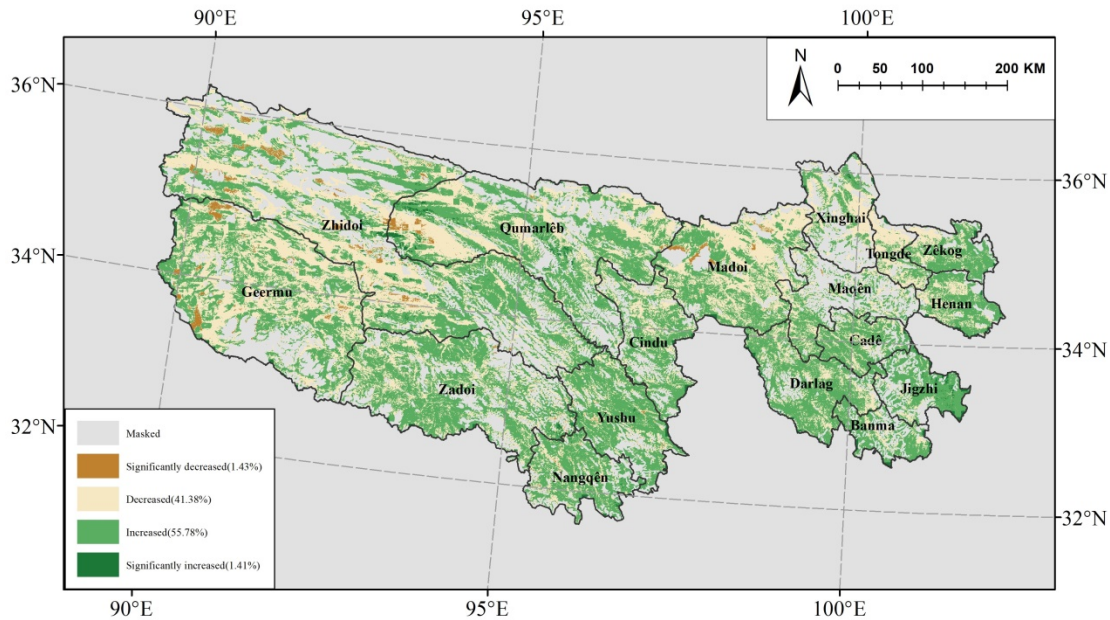
375 Fig.5. Change trend from 1982 to 2012 for the IMF

376 Change trend from 1982 to 2012 for the IMF is shown in Fig. 5. It shows that from 1982 to 2012 the IMF
 377 in TRHR showing an overall increase trend. The percentage of significantly increased IMF is 45.07%, which
 378 cover the largest area of the TRHR, while the percentage of insignificantly increased is 10.67%; the percentage
 379 of significantly decreased IMF from 1982 to 2012 is 34.34%, cover the secondary largest area of the TRHR, and
 380 the percentage of insignificantly decreased IMF is 9.92%.

381 The IMF in the TRHR shows a trend of decreasing gradually from southeast to northwest. The meteorological
 382 conditions in the northwest were relatively poor, and the vegetation growth was relatively poor. Areas where the
 383 cumulative NDVI and climatic factors have established an effective model account for 75.65% ($P < 0.01$), and
 384 91.427% ($P < 0.05$) of the total area of grassland. This indicates that apart from the meteorological elements
 385 listed in this article, human activities could have an impact on the growth of grassland vegetation in these areas.
 386 In the study area, the time series mean of the accumulated NDVI showed inter-annual fluctuations from 1982 to
 387 2012 during the growing season. Overall, NDVI presents a situation where increasing and decreasing coexist.
 388 The IMF showed a similar changing characteristic. The change trends of the accumulated NDVI and IMF are
 389 similar in large spatial patterns, illustrating that the climate factors contribute a large part to the NDVI change in
 390 the TRHR. But there are differences between them in local areas (Please look carefully at Figure 4 and Figure 5).
 391 In addition, the area ratio of each change level is also different.

392 Change trend from 1982 to 2012 for the NCUE is shown in Fig. 6. It indicates that from 1982 to 2012 the
 393 NCUE in TRHR showing an overall increase trend. The percentage of significantly increased NCUE is 1.41%,

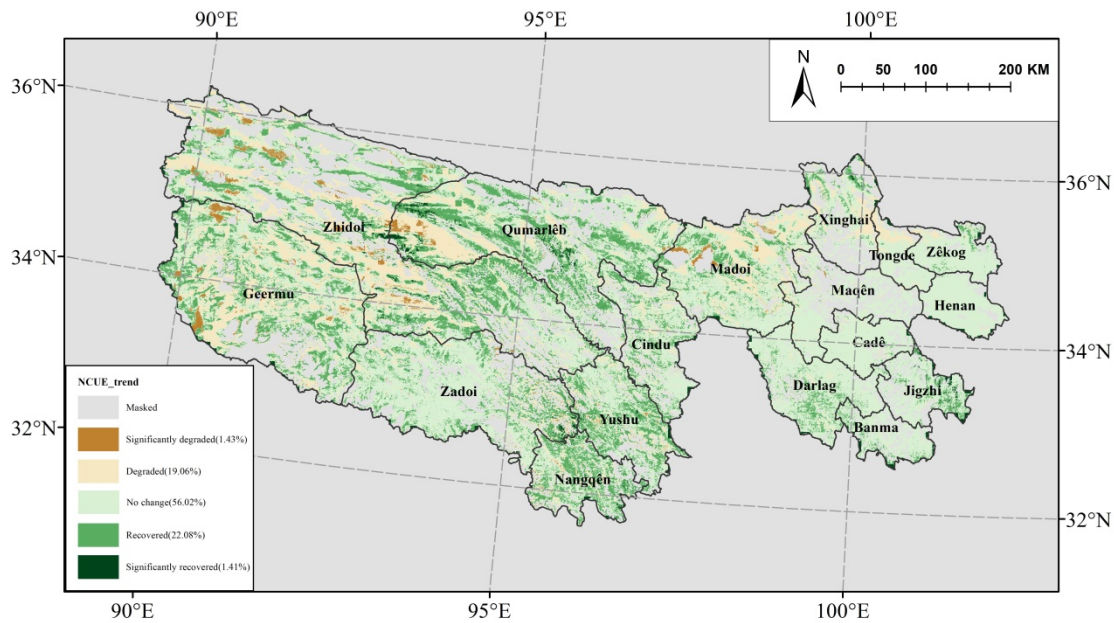
394 which cover the smallest area of the TRHR, while the percentage of insignificantly increased is 55.78%. The
 395 percentage of significantly decreased NCUE from 1982 to 2012 is 1.43%, which also covers the smallest area of
 396 the TRHR; the percentage of insignificantly decreased NCUE is 41.38%, which is the second largest proportion.
 397 The spatial distribution pattern for NCUE is similar to that of NDVI and IMF.



398
 399 Fig.6. Change trend from 1982 to 2012 for the NCUE

400 *4.2 Spatial distribution characteristics of grassland degradation and restoration*

401 The spatial distribution of grassland changes from 1982 to 2012 determined by the temporal trends of NCUE is shown
 402 in Fig. 7. In this figure, the degraded grassland in the study area accounted for 20.49% of the total area of grassland.
 403 Among these areas, significant degradation accounts for 1.43% ($P < 0.05$), and degradation but not significant accounted
 404 for 19.06%. Grassland restoration accounts for 23.49% of the total grassland area. Significant recovery accounts for
 405 1.41%, and recovery but not significant accounts for 22.08%. Grassland basically unchanged area accounts for 56.02% of
 406 the total grassland area.



407

408 Fig.7. Spatial distribution characteristic of grassland degradation and restoration from 1982 to 2012 by NCUE trend

409 The above trend analysis shows that in the past 31 years, the status of the grassland in TRHR has improved. Grassland
 410 ecosystems in some areas show a recovery trend, but there are still some areas that continue to deteriorate. The spatial
 411 distribution includes: (1) In Central Yushu County and Nangqên County, a large area of grassland restoration appears.
 412 Towards Cindu County, Qumarlêb County and Zadoi County, the grassland restoration also happens; (2) the southeast of
 413 Jigzhi County, south of Darlag County, Xinghai county recovery is significant; (3) Grassland degradation was mainly
 414 distributed in the northeast of Madoi County, west of Qumarlêb and Zhidoi County, as well as the Geermu local area.
 415 Grassland restoration also exists in these areas.

416 *4.3 Comparison and analysis of grassland degradation and restoration results*

417 The results achieved in this paper are compared and analyzed with LUCC, trend of the accumulated NDVI during the
 418 growing season, and field observation data obtained in 2013 (56 samples) and 2009 (70 samples), as shown in Table 3
 419 and Table 4. From the tables, we can see that: (1) areas with negative NCUE slopes usually correspond to grassland
 420 with different degrees of degradation observed in the field and (2) the NCUE slope of the non-degenerated areas
 421 observed in the field is mostly positive. The ratio in both cases is about 68% (denoted by Y in Table 3 and Table 4). This
 422 shows that there might be some connections between the changing trends and field observed grassland degradation
 423 status.

424 For non-degraded grasslands observed in the field, there are three types of trends of the NCUE. One is positive, which
 425 means that the areas are restored from grasslands with different degrees of degradation or the areas with non-degraded
 426 grassland. The second type is remaining unchanged. The last is negative, such as the healthy grassland area that has

427 undergone slight degradation but still belongs to an un-degraded level. Table 3 and Table 4 show that many sites belong to
 428 the first case.

429 Areas with positive or almost constantly changing trends are not necessarily the un-degraded grasslands, and they could
 430 be recovered from grasslands with different levels of degradation. For example, for point 21 (35.00939 N, 97.59611 E) in
 431 Table 3, the NCUE trend value is 0.005, indicating that the grassland was recovering during the 31 years, and the
 432 changing trend of the LULC also shows that from 1990 to 1995, the point changed from sandy land to moderately
 433 covered grassland, and there has been no change thereafter. The grassland at this point tends to recover. However,
 434 moderately degraded grasslands were observed in the field. The actual situation is that the area has recovered from
 435 extremely degraded sandy lands, rather than degraded from lightly degraded or un-degraded grasslands.

436 The monitoring results of this study were also compared and analyzed with the change trend of the LULC and the
 437 accumulated NDVI (See Table 5 for the results). Due to more than 70% of the NDVI change trend is a significant
 438 change, this paper does not define the level of unchanged grassland by using NDVI. Therefore, the points where the
 439 LULC is unchanged are not considered (such as points 1, 12, etc. with a gray background in Table 3). In addition, some
 440 points whose trends of LULC type changes cannot clearly judged (such as points 4, 20, etc. in bold, italic and underlined
 441 font) are also removed. In the end, the samples compared with LULC were 25 in 2013 and 39 in 2009. The samples
 442 compared with NDVI and field observation were 56 in 2013 and 70 in 2009. Detailed information and comparison of
 443 results are shown in Table 3, Table 4 and Table 5.

444 Table 3 Comparison of grassland changes detected by NCUE with field-observation data, LULC and NDVI change trend in 2013

ID	Latitude	Longitude	FODS	A	B	C	D	E	NDVI_S	NCUE_S	R1	R2	R3	R4	R5
<u>1</u>	<u>35.35564</u>	<u>99.21936</u>	<u>I</u>	<u>UC</u>	<u>UC</u>	<u>UC</u>	<u>UC</u>	<u>UC</u>	<u>-0.003841715</u>	<u>-0.001691300</u>				<u>Y</u>	
2	35.35817	99.14418	II	UC	MC to BL	UC	UC	DE	-0.008705663	-0.010987038	Y	Y	Y	Y	Y
3	35.35122	99.11633	II	UC	BL to LC	UC	UC	RE	-0.009034017	-0.013418230	Y		Y	Y	
<u>4</u>	<u>35.34777</u>	<u>99.10384</u>	<u>II</u>	<u>LC to MC</u>	<u>MC to BL</u>	<u>UC</u>	<u>UC</u>		<u>-0.008628733</u>	<u>-0.011451510</u>	<u>Y</u>		<u>Y</u>	<u>Y</u>	
5	35.35819	99.14449	II	UC	MC to BL	UC	UC	DE	-0.007854215	-0.010987038	Y	Y	Y	Y	Y
6	35.35778	99.14461	III	UC	MC to BL	UC	UC	DE	-0.007854215	-0.008911362	Y	Y	Y	Y	Y
7	35.35569	99.14528	III	UC	MC to BL	UC	UC	DE	-0.00627514	-0.008911362	Y	Y	Y	Y	Y
8	35.35571	99.14529	III	UC	MC to BL	UC	UC	DE	-0.00627514	-0.008911362	Y	Y	Y	Y	Y
9	35.35563	99.14528	III	UC	MC to BL	UC	UC	DE	-0.00627514	-0.008812329	Y	Y	Y	Y	Y
10	35.35572	99.14535	III	UC	MC to BL	UC	UC	DE	-0.00627514	-0.008911362	Y	Y	Y	Y	Y
11	35.3559	99.14506	II	UC	MC to BL	UC	UC	DE	-0.00627514	-0.008911362	Y	Y	Y	Y	Y
<u>12</u>	<u>35.33887</u>	<u>99.07852</u>	<u>II</u>	<u>UC</u>	<u>UC</u>	<u>UC</u>	<u>UC</u>	<u>UC</u>	<u>-0.009069584</u>	<u>-0.018127525</u>	<u>Y</u>		<u>Y</u>	<u>Y</u>	
<u>13</u>	<u>35.33831</u>	<u>99.07593</u>	<u>II</u>	<u>UC</u>	<u>UC</u>	<u>UC</u>	<u>UC</u>	<u>UC</u>	<u>-0.009252124</u>	<u>-0.009877190</u>	<u>Y</u>		<u>Y</u>	<u>Y</u>	
<u>14</u>	<u>35.33889</u>	<u>99.07623</u>	<u>III</u>	<u>UC</u>	<u>UC</u>	<u>UC</u>	<u>UC</u>	<u>UC</u>	<u>-0.009252124</u>	<u>-0.009877190</u>	<u>Y</u>		<u>Y</u>	<u>Y</u>	
<u>15</u>	<u>35.33104</u>	<u>99.06526</u>	<u>II</u>	<u>UC</u>	<u>UC</u>	<u>UC</u>	<u>UC</u>	<u>UC</u>	<u>-0.008830147</u>	<u>-0.015823964</u>	<u>Y</u>		<u>Y</u>	<u>Y</u>	
<u>16</u>	<u>35.11447</u>	<u>97.88955</u>	<u>II</u>	<u>UC</u>	<u>UC</u>	<u>UC</u>	<u>UC</u>	<u>UC</u>	<u>-0.004332194</u>	<u>-0.012704480</u>	<u>Y</u>		<u>Y</u>	<u>Y</u>	
17	35.11191	97.84891	III	UC	MC to LC	UC	UC	DE	-0.001321627	0.0004284080				Y	Y
18	35.11121	97.82476	III	MC to LC	UC	UC	UC	DE	-0.001073083	-0.002376339	Y	Y	Y	Y	Y
19	35.11119	97.82474	II	MC to LC	UC	UC	UC	DE	-0.001073083	-0.002376339	Y	Y	Y	Y	Y
<u>20</u>	<u>35.08346</u>	<u>97.74453</u>	<u>II</u>	<u>UC</u>	<u>MC to Lake</u>	<u>UC</u>	<u>UC</u>		<u>-0.000317136</u>	<u>0.0146827520</u>				<u>Y</u>	

21	35.00939	97.59611	III	S to MC	UC	UC	UC	RE	-0.000360983	0.0050489130	Y	Y
22	34.90438	97.53104	II	MC to LC	LC to S	UC	UC	DE	0.004509227	0.0130356370	Y	
23	34.90376	97.53127	II	MC to LC	UC	UC	UC	DE	0.004844830	0.0138548820	Y	
<u>24</u>	<u>34.90145</u>	<u>97.55336</u>	<u>II</u>	<u>LC to S</u>	<u>UC</u>	<u>UC</u>	<u>S to LC</u>	<u>0.000522814</u>	<u>-0.034139626</u>	<u>Y</u>		
25	34.89037	97.53186	II	UC	UC	UC	S to LC	RE	0.000201392	-0.044988625	Y	Y
26	35.0956	97.96458	II	UC	UC	UC	UC	UC	0.001784259	0.011186769	Y	Y
27	34.77374	98.125	I	LC to MC	UC	UC	UC	RE	0.004216325	0.032453351	Y	Y
<u>28</u>	<u>34.64989</u>	<u>98.04014</u>	<u>I</u>	<u>LAKE to MC</u>	<u>MC to Lake</u>	<u>UC</u>	<u>UC</u>	<u>0.001121222</u>	<u>0.017450565</u>	<u>Y</u>	<u>Y</u>	<u>Y</u>
29	35.2203	98.96438	I	UC	LC to MC	UC	UC	RE	0.000573364	-0.007723934	Y	Y
30	34.63899	98.02946	I	UC	UC	UC	UC	UC	0.003921086	-0.031985901	Y	Y
31	34.46087	97.95137	III	UC	UC	UC	UC	UC	-0.007523185	-0.016297076	Y	Y
32	34.127	97.65768	I	LC to MC	UC	UC	UC	RE	-0.001505453	0.011327818	Y	Y
33	34.07806	97.61038	I	UC	UC	UC	UC	UC	0.005463828	0.009898725	Y	Y
34	33.20103	97.46926	II	UC	MC to LC	UC	UC	DE	-0.00019945	0.002483916	Y	Y
35	33.00867	97.24764	I	UC	BL to LC	UC	UC	RE	-0.012522309	-0.01971980	Y	
36	32.79402	97.19837	II	HC to MC	UC	UC	UC	DE	0.006866030	-0.002596253	Y	Y
37	32.84219	97.0757	II	UC	UC	UC	UC	UC	-0.002822498	-0.005253023	Y	Y
38	32.84219	97.0756	III	UC	UC	UC	UC	UC	-0.002822498	-0.005253023	Y	Y
39	33.12565	96.70239	II	UC	UC	UC	UC	UC	0.0013622580	0.000200635	Y	Y
<u>40</u>	<u>33.20386</u>	<u>96.56449</u>	<u>I</u>	<u>UC</u>	<u>MC to Lake</u>	<u>UC</u>	<u>UC</u>	<u>0.002574169</u>	<u>0.004603553</u>	<u>Y</u>	<u>Y</u>	<u>Y</u>
41	33.83283	95.69785	I	UC	UC	UC	UC	UC	-0.004609005	0.004329267	Y	Y
<u>42</u>	<u>33.82198</u>	<u>95.68428</u>	<u>II</u>	<u>LC to BL</u>	<u>BL to LC</u>	<u>UC</u>	<u>UC</u>	<u>-0.000663235</u>	<u>0.015286485</u>	<u>Y</u>	<u>Y</u>	<u>Y</u>
<u>43</u>	<u>33.7959</u>	<u>95.72888</u>	<u>II</u>	<u>LC to MC</u>	<u>MC to LC</u>	<u>UC</u>	<u>UC</u>	<u>0.004994782</u>	<u>0.004361200</u>	<u>Y</u>	<u>Y</u>	<u>Y</u>
44	33.80899	95.71709	II	UC	UC	UC	UC	UC	0.002417488	0.042501174	Y	Y
45	33.80882	95.71704	II	UC	UC	UC	UC	UC	0.002417488	0.042501174	Y	Y
46	33.80893	95.71697	I	UC	UC	UC	UC	UC	0.002417488	0.042501174	Y	Y
47	33.95369	95.70775	II	UC	MC to LC	UC	UC	DE	-0.002750233	-0.011134764	Y	Y
48	33.99134	95.7685	I	BL to MC	UC	UC	UC	RE	-0.006056834	0.008117074	Y	Y
49	33.99133	95.76849	I	BL to MC	UC	UC	UC	RE	-0.006056834	0.008117074	Y	Y
<u>50</u>	<u>34.01324</u>	<u>95.81013</u>	<u>II</u>	<u>MC to HC</u>	<u>HC to MC</u>	<u>UC</u>	<u>UC</u>	<u>-0.004104727</u>	<u>-0.005211535</u>	<u>Y</u>	<u>Y</u>	<u>Y</u>
<u>51</u>	<u>34.06713</u>	<u>95.8216</u>	<u>I</u>	<u>LC to HC</u>	<u>HC to LC</u>	<u>UC</u>	<u>UC</u>	<u>0.003387089</u>	<u>-0.003873405</u>	<u>Y</u>	<u>Y</u>	<u>Y</u>
<u>52</u>	<u>34.10863</u>	<u>95.81035</u>	<u>I</u>	<u>MC to HC</u>	<u>HC to BL</u>	<u>BL to MC</u>	<u>UC</u>	<u>-0.00202559</u>	<u>0.016639065</u>	<u>Y</u>	<u>Y</u>	<u>Y</u>
<u>53</u>	<u>34.11975</u>	<u>95.78966</u>	<u>II</u>	<u>MC to HC</u>	<u>HC to MC</u>	<u>UC</u>	<u>UC</u>	<u>-0.003015237</u>	<u>0.000939846</u>	<u>Y</u>	<u>Y</u>	<u>Y</u>
<u>54</u>	<u>34.11925</u>	<u>95.78921</u>	<u>I</u>	<u>MC to HC</u>	<u>HC to MC</u>	<u>UC</u>	<u>UC</u>	<u>-0.000904993</u>	<u>0.000939846</u>	<u>Y</u>	<u>Y</u>	<u>Y</u>
<u>55</u>	<u>034.13905</u>	<u>95.81607</u>	<u>II</u>	<u>BL to HC</u>	<u>HC to LC</u>	<u>UC</u>	<u>UC</u>	<u>-0.011553417</u>	<u>-0.014404091</u>	<u>Y</u>	<u>Y</u>	<u>Y</u>
<u>56</u>	<u>34.13008</u>	<u>95.84046</u>	<u>I</u>	<u>Non-grass</u>	<u>UC</u>	<u>UC</u>	<u>UC</u>	<u>-0.003641036</u>	<u>-0.002743170</u>	<u>Y</u>	<u>Y</u>	<u>Y</u>

445 (Here: Y means match; FODS: Field observed degradation situation; NCUE_S: Slope of NCUE; NDVI_S: Slope of NDVI; I means not degenerate;
446 II means mildly degenerate; III means moderately degenerate; UC means essentially constant or unchanging; DE means degradation; RE
447 means recover; BL means bare land; LC means lower coverage; MC means moderate coverage; S means sand; HC means high coverage; WL means
448 wetland; BF means bush forest; and S to MC means sand land that has been turned to moderate coverage grassland, and so forth. A: 1990-1995
449 LULC change; B: 1995-2000 LULC change; C: 2000-2005 LULC change; D: 2005-2010 LULC change; E: 1990-2010 LULC change; R1: results of
450 comparison of NCUE and FODS; R2: results of comparison of NCUE and LULC; R3: results of comparison of NUCE and NDVI. R4: results of
451 comparison of NDVI and FODS; R5: results of comparison of NDVI and LUCC.)

452
453 Table 3 shows the information of all points and the results of the comparative analysis in 2013. The points with gray
454 background are the ones where the land use type does not change during the 1990-2010. Points which cannot express the
455 trends of LULC type changes clearly are shown in bold, italic, and underlined fonts.

456 Table 4 Comparison of grassland changes detected by NCUE with field-observation data, LUCC and NDVI change trend in 2009
 457 (partly listed)

I D	Latitud e	Longitud e	Field description	F	A	B	C	D	G	NDVI_S	NCUE_S	R 1	R 2	R 3	R 4	R 5
1	34.3639 7	95.68698	black soil beach	UC	UC	UC	UC	UC		-0.006070 5	-0.009872 8	Y		Y	Y	
2	33.7710 7	95.7997	black soil beach	MC to LC	LC to MC	UC	UC	UC		0.0029256	0.0141897			Y		
3	32.8909 8	96.7422	small patches of black soil beach	UC	UC	UC	UC	UC		-0.005256	-0.004025 5	Y		Y	Y	
4	32.8978 8	96.63175	typical meadow, medium coverage	UC	UC	M C to LC	UC	UC	D E	-0.003311 3	-0.001583 1	Y	Y	Y	Y	Y
5	33.8212 2	97.14615	alpine meadow, partly wetland, medium coverage	M C to LC	UC	UC	UC	UC	D E	-0.005047 8	-0.004051 6	Y	Y	Y	Y	Y
6	33.8500 3	97.19395	black soil beach on both sides of the road is more serious, there are small rivers	LC to MC	MC to BL	BL to LC	UC	UC		-0.002888 5	-0.007000 2	Y		Y	Y	
7	33.9253 8	97.28777	grassland degradation is severe, and there are swamp meadow	UC	UC	UC	UC	UC		-0.000613 7	-0.005249 4	Y		Y	Y	
8	33.9303 2	97.29348	to the left of the road are large tracts of rat holes and early black soil beach	M C to LC	UC	UC	UC	UC	D E	0.0016295	-0.010180 9	Y	Y			
9	33.9378	97.30743	on the left side of the road is a swamp meadow, medium coverage	UC	MC to LC	LC to MC	UC	UC		0.0005539	-0.006524 7	Y				
10	33.9572 7	97.3297	on the right side of the road, there is a swamp meadow and a small river, medium coverage	MC to LC	LC to MC	UC	UC	UC		0.0005126	-0.005760 3	Y				

458 (Here: Points in bold font are LUCC comparison points. F means LULC change from 1980-1990; G means LULC change from 1980-2010;
 459 “black soil beach” means extremely degraded grassland.)

460 The comparative analysis results of the two periods in 2009 and 2013 are shown in Table 5. From Table 5, it is found
 461 that the performance of NCUE is better than that of NDVI. Comparison with Field observed degradation situation, the
 462 performance of NCUE and NDVI is similar; For LUCC, the performance of NCUE is better than that of NDVI. The
 463 positive and negative change trend consistency between NDVI and NCUE is about 70%.

464 Table 5 Comparative analysis consistency of changing trends in 2009 and 2013

2013				2009			
	FODS	LULC	NDVI		FODS	LULC	NDVI
NCUE	66.07%	68.00%	67.86%	NCUE	70.51%	69.23%	71.79%
NDVI	60.71%	64.00%		NDVI	71.85%	46.15%	

465

466 From Fig.4 and Fig.6, we can see that from the perspective of the positive and negative trends of the overall grassland
467 change, the spatial distribution characteristic of NDVI and NCUE is similar. Yet, the biggest differences of change trends
468 between NDVI and NCUE are that NDVI detects more than 70% of the grassland showing significant changes, while
469 NCUE only detects no more than 3%, and most of the areas are basically unchanged or in a state of insignificant changes.
470 It shows that NDVI is sensitive to climate fluctuations, but NCUE overcomes the influence of climate fluctuations,
471 reflecting the change of grassland being affected by human activities and long-term climate change. The grassland
472 change detection result of NCUE is close to the existing researches (Wu et al. (2014); QUAYE-BALLARD, J.A. (2014)),
473 yet the detection result of NDVI is completely different. Furthermore, it is found that counties in the east of TRHR
474 showing large area grassland recovery in Fig.6, but these areas belong to basically unchanged type shown in Fig.7. This
475 shows that the degree of insignificant restoration of grassland in the eastern part of the study area is lower than that of
476 other place (such as Yushu), and the change is small over a long period of time, which is approximately unchanged.

477 **5. Discussions**

478 *5.1 The characteristics of annual changes of major climatic factors and climatic factors selected*

479 Thirteen meteorological stations in the study area were used to analyze statically the trends of the monthly average
480 temperature, accumulation of rainfall, average hours of sunshine, average wind speed, etc. from 1982 to 2012. It was
481 found that the annual average temperature of TRHR between 1982 to 2012 was $-0.25\text{ }^{\circ}\text{C}$ and it continued to increase at
482 the rate of $0.59\text{ }^{\circ}\text{C}/10\text{a}$. The rising trend of the annual average temperature passed the significant test ($p<0.001$). Rainfall
483 had significant inter-annual variations, and the overall increase was weak. Rainfall was mainly concentrated during the
484 growing season, accounting for 82.3% of the rain throughout the whole year. The average hours of annual sunshine and
485 the one during the growing season fluctuate greatly, and the overall trends are decreasing. These passed the significant
486 level test ($p<0.05$). The annual average wind speed and the one during the growing season show clear downward trends
487 and pass the significant test ($p<0.001$). The average annual surface temperature and the one during the growing season
488 showed significant upward trends ($p<0.001$) from 1982 to 2012. In 1994, the surface temperature changed from cold to
489 warm, and beyond 1997, it presents a clear increasing trend (Sun, 2015).

490 The thirteen meteorological factors selected based on the data from weather stations and Pearson correlation analysis are
491 as follows: the sum of the precipitation during the growing season, the average of the temperature, sunshine hours,
492 surface temperature, and wind speed of growing season; three hysteresis effect factors including the average temperature
493 in April, the average wind speed in March and the average surface temperature in February; and other factors including
494 an annual accumulated temperature of greater than 0°C , the growth season rainfall condition index, the temperature

495 condition index, the sunshine conditions index and the STPC index. Freeze and thaw are important factor that affect the
496 soil moisture in the TRHR region, and they will be considered in future study.

497 *5.2 The modeling effect of the IMF*

498 Multiple linear stepwise regression (backward mode) and five climatic factors of the growing season, including the
499 accumulative precipitation, average temperature, average sunshine, average land surface temperature and average wind
500 speed, excluding time-lag effects, were used in the model, and the effective model is established on each weather station.
501 On average, the correlation coefficient was 0.53 with low estimation accuracy. A more effective model could be
502 established for each site after adding time-lag effects and hydrothermal combinations of variables. The correlation
503 coefficient could reach 0.68 on average.

504 By performing multiple stepwise linear regressions, taking the NDVI as a dependent variable and climate factors as
505 independent variables, it was found that the incorporation of more independent variables does not necessarily produce a
506 good modeling effect. Too many parameters could cause overfitting and collinearity problems among different variables,
507 while too few will also affect the modeling accuracy. When the multivariate regression was employed with the "Enter"
508 mode, it was found that the majority of sites were unable to establish an effective model of the accumulated NDVI and
509 climatic elements. In contrast, Stepwise regression could establish the relevant model effectively, and it passed the
510 significant level test ($p < 0.05$ at 95% confidence interval). The few factors selected during the modeling process could
511 reflect the major factors, but the modeling accuracy is relatively low, with the average correlation coefficient of 0.48
512 only. "Backward" mode selects moderate parameters with high modeling accuracy. However, there are some sites with
513 too many parameters, while some of the independent variables were strongly correlated. It is worth paying attention to
514 the choice of the appropriate number of factors to reach a high precision of modeling without overfitting to avoid
515 collinearity. After the first multiple linear regression we will check the collinearity problem, such as whether the VIF
516 (Variance Inflation Factor) is greater than 10 or the Condition Index is greater than 30. If these situations occur, then the
517 independent variable corresponding to the largest VIF or the Condition Index will be removed. The remaining
518 independent variables will be used for the re-regression. This can solve the problem of collinearity between independent
519 variables. Experiments in meteorological stations illustrate the effectiveness of the method.

520 *5.3 Analysis of effectiveness of NCUE*

521
522
523
524
525
526

527
528
529
530
531
532
533
534
535
536
537
538
539
540
541
542
543
544
545
546
547
548
549
550
551
552
553
554
555
556
557
558
559
560

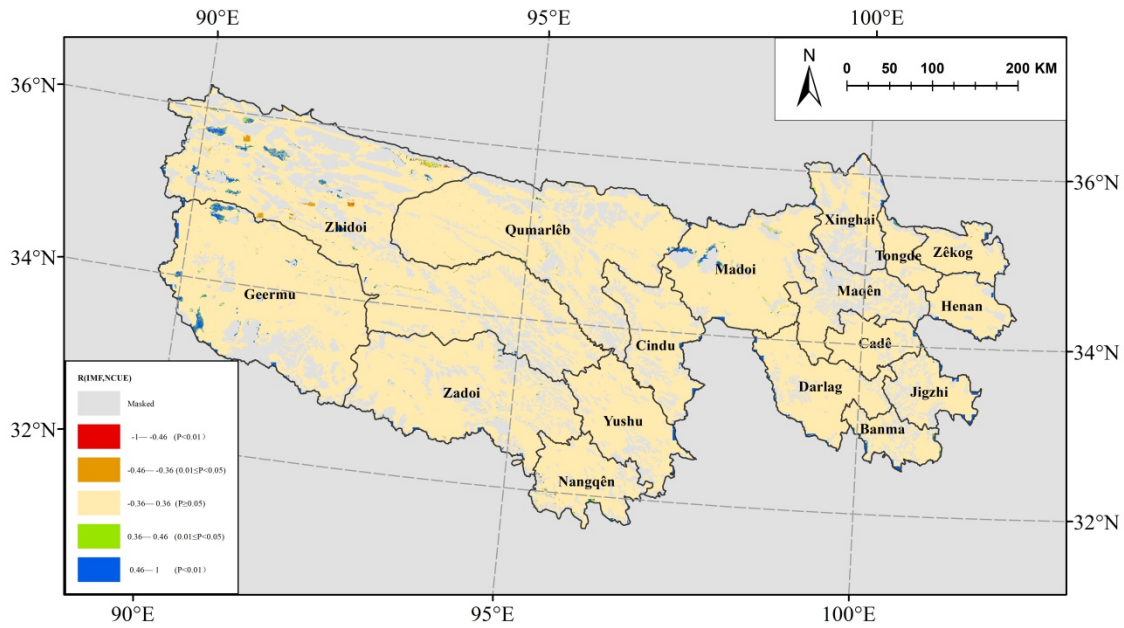


Fig. 8. Correlation coefficient and significance test between NCUE and IMF

Correlation analysis was carried out between each factor within the NCUE to illustrate that the NCUE presented in this paper is effective for reducing climatic fluctuation. The spatial distribution of the correlation coefficient between the NCUE and IMF is shown in Fig. 8. It was found that the correlation between the NCUE and IMF was weak, and in most areas, their correlation did not pass the significant test of 0.05. This result shows that NCUE can reduce the influence of climate fluctuation. The correlation between the cumulative NDVI during the growing season and the IMF was high, and the NDVI is greatly affected by the climate. The correlation between the cumulative NDVI and the NCUE during the growing season was also significant, and the NCUE can reflect vegetation growth well, which is not sensitive to climate fluctuations.

5.4 Credibility analysis of the results of detected grassland changes

The results were comparatively analyzed using field surveys, LUCC and NDVI changes. Four kinds of grassland change data can be used for comparative analysis. These can reflect the states and changes in grassland vegetation. The long-term changes of grassland observed through field surveys are conceptually different from the monitoring of grassland degradation in this paper. However, there might be some relationships between the results of the changes and the process of the changes. Therefore, there may be some rationality behind the analysis and comparison.

It is feasible to perform a comparative analysis using the five sets of LULC changes because there is consistency in the classification definitions. There are some differences in the essence between these four kinds of grassland change detection methods (which are field survey, LUCC comparison, NDVI and NCUE), and this will produce a certain uncertainty in the analysis results. Observations in the field are the result of long-term changes in grassland. The

561 coverage and community structure information were considered in the classification of the grassland degradation level,
562 reflecting the objective reality of the degraded grassland.

563 The NCUE slope reflects the long-term trends of vegetation growth after reducing the impact of climate fluctuation. The
564 LULC changes also reflect the long-term trends of vegetation growth. The change of the total vegetation cover does not
565 reflect the changes in the community structure and does not take the impact of climate fluctuation into account. In
566 addition, the LULC data is obtained from visual interpretation through human-computer interactions. The complexity of
567 natural phenomena, such as grassland degradation, as well as the domain knowledge and the subjectivity of the
568 interpreter, may all lead to uncertainty in the identification. Due to the lack of long-term fixed-point field observation
569 data and certain errors in the various types of data used in the analysis, the results present some uncertainties. It is
570 necessary to obtain more reliable data to strengthen the analysis and verification of the results. Additionally, the size of
571 the field survey samples is 30×30 square meters. Since the pixel size used in this paper is 250×250 square meters, there
572 might be some discrepancies caused by the inconsistency in spatial scales when analyzing based on field observations.

573 The research found that the correlation between the cumulative NDVI and cumulative rainfall is very weak at pixel scale,
574 so the RUE index that only considers rainfall factors may not characterize NDVI well. Therefore, the RUE and the
575 Residual Index derived by RUE are also not used in this article. This article compares the temporal trends of cumulative
576 NDVI during the growing season and NCUE.

577 A comparison with some previous studies of the grassland restoration and degradation in TRHR are shown in Table 6.
578 The period of these studies is close to or partially overlaps with this study.

579 Table 6 some previous studies of the grassland restoration and degradation in TRHR

Reference	Indicators	Time span	Remote sensing data	Results of grassland restoration and degradation
This study	NUCE	1982-2012	NOAA / AVHRR-NDVI MODIS-NDVI	Overall trend: a slightly recovery trend. Degradation concentrated distribution areas: northeast of Maduo, midwest of Qumarlêb and Zhidoi and the Geermu local area, et al. Restoration concentrated distribution areas: In the central Yushu and Nangqên County, Qumarlêb, Zhidoi, Zadoi County, et al.; the southeast of TRHR, such as Jigzhi, Darlag et al.
Liu et al.(2008)	Coverage change rate, grassland fragmentation, etc.	Mid to late 1970s, early 1990s, 2004	MSS, TM, TM/ETM	Overall trend: the continued process of grassland degradation. Degradation concentrated distribution areas: Qumarlêb, Chenduo, Maduo, et al. Restoration concentrated distribution areas: in Zadoi and Tanggula Mountain Township, the grassland has local improvement areas.
Wu et al.(2014)	reference vegetation coverage	1981-2006	NOAA / AVHRR-NDVI	Overall trend: no major development in grassland degradation since 1980s. After 2000, the grassland degradation trend was slowed down initially. Degradation concentrated distribution areas: Zadoi, Dari, Qumarlêb, Tanggula Mountain Township, Xinghai, Maduo, et al. Less degraded areas: Gander, Zeku, Henan, Tongde, et al.
QUAYE-BALLARD, J.A. (2014)	A5 time series produced by Multi-Resolution Analysis	1981-2012	NOAA / AVHRR-NDVI MODIS-NDVI	Overall trend: The total ratios of the positive and negative slopes are 69.6% and 30.4%. Degradation concentrated distribution areas: Qumarlêb, Chenduo, Maduo, et al.

	(MRA) of Wavelet Transform			Restoration concentrated distribution areas: in Zaduo and Tanggula Mountain Township, the grassland has local improvement areas.
Shen et al.(2018)	Detecting Breakpoints and Estimating Segments in Trend (DBEST)	2000-2015	MODIS-NDVI	Overall trend: recovery of the vegetation. Degradation concentrated distribution areas: Maduo, Zadoi, Nangqên, Jiuzhi and Zhidoi , et al. Restoration concentrated distribution areas: the southeastern TRHR, including Xinghai, Tongde, Zeku, as well as the middle regions, such as Chengduo and Yushu, et al.

580 It is found that the grassland showed a recovery trend in this study, and which is basically consistent with that of Wu et
581 al. (2014), Quaye-Ballardq (2014), and Shen et al. (2018). The proportions of unchanged and significantly change
582 grassland are similar to that of Quaye-Ballardq (2014). Degradation area is between that of Liu et al. (2008) and Wu et
583 al. (2014). Restoration area in this study is slightly higher than that of 1990s - 2000s later (Wu et al., 2014). For
584 degradation concentrated distribution areas in the paper, there is more overlap with the conclusions of other studies.
585 Restoration concentrated distribution areas are similar to that of Wu et al. (2014) and Shen et al. (2018).

586 Form Table 6, it is found that there is a certain degree of difference between the results of the various studies because
587 of different grassland degradation indicators, method mechanism, research periods, and data accuracy, etc. These
588 differences should hinder the comparison between the results of different studies in the same area.

589 Weeds may hide the severity of grassland degradation when using the NDVI method. Grassland degradation is shown not
590 only as a decrease in biomass or coverage but also as changes in the composition of the community. In the early stage of
591 grassland degradation, obvious changes of biomass usually do not occur, but there are changes in the community
592 structure, where the reduction of dominant native grass species appears with the increase of poisonous weeds. In some
593 severely degraded areas, the vegetation coverage is low, and there are large areas of bare land. However, in other
594 severely degraded areas, a large number of poisonous weeds may grow with high coverage. Using the grassland NDVI
595 alone as a deteriorating indicator, it will be impossible to distinguish between these situations. A field investigation found
596 that poisonous weeds breed quickly in the TRHR. They also mix with native plant species. Poisonous weeds grow well
597 and cover large areas of vegetation in the extremely degraded "Black Earth Beach" area, and few native plant species
598 exist. This type of situation will cover up the actual degree of grassland degradation and lead to uncertainty in the
599 monitoring of grassland degradation using the NDVI time series method.

600 **6 Conclusion**

601 Inspired by the RUE and based on the climate characteristics of the study area, a novel grassland ecosystem
602 characteristic index, the NCUE, was proposed in this paper through the comprehensive consideration of major climatic
603 factors affecting the growth of grassland vegetation, such as light, temperature, and water, using multi-source geospatial
604 data. The model was adapted for the monitoring of grassland changes in the study area and could reduce the influence of

605 climate fluctuations. Through analysis and comparison with actual observed data, land use/cover data and NDVI, the
606 NCUE index was shown to be effective in monitoring grassland changes.

607 Most of the grasslands in the TRHR have shown insignificantly changes in the past 31 years. At the same time, grassland
608 degradation and restoration co-exist, and the area of degraded grassland is slightly less than that of restored grassland. In
609 terms of spatial distribution in grassland changes, there is a trend of restoration in the southeast and middle region and
610 degradation in the northwest based on the positive and negative change trends. There are large areas of grassland
611 restoration in the southeastern part of Jiuzhi, Darlag Counties, as well as in Yushu, Nangqian, Qumarlêb and Zhidoi
612 Counties in the TRHR. Grassland degradation is mainly distributed in the northeast of Maduo County and the central and
613 western parts of Zhidu County, Qumarlêb, and Golmud. The NCUE might be applied in similar arid and semi-arid alpine
614 grassland areas (such as in Gansu Province, the Ningxia Hui Autonomous Region, the Tibet Autonomous Region, etc.).
615 Due to the cold weather and harsh natural conditions in this area, it is difficult to conduct field surveys. Due to the lack of
616 long-term fix-point field observation data and the various data used for the analysis, the results may present some
617 uncertainty. We should further acquire more reliable data sources to strengthen the analysis and verification of
618 monitoring results. In the future, we would like to strengthen the research of information extraction on large-scale weeds
619 and perform more scientific monitoring of grassland degradation. The reason and mechanism of grassland degradation in
620 this area should further be studied to evaluate the effectiveness of environmental protection and human activities
621 objectively. Grassland degradation can also cause soil degradation and even desertification; changes in grassland seed
622 bank and soil properties, such as soil water content, soil organic carbon, total nitrogen and soil bulk density, soil
623 microorganisms, soil enzyme, etc. In the future, we can also conduct research on soil degradation, desertification, and
624 changes in soil moisture caused by grassland degradation with the help of remote sensing technology.

625 **Acknowledgments**

626 This work is supported by the National Nature Science Foundation of China (No. 41271361; 41871326). The
627 authors would like to express sincere gratitude to X.Z. Feng from the Nanjing University, J.Y. Liu, Q.Q. Shao,
628 J.W. Fan from the Institute of Geography Sciences and Natural Resources Research (CAS), and Y. Wang from
629 the University of Warwick, UK for their suggestions and assistance with the provision of research data.

630 **References**

631 An, R., Wang, H.L., Feng, X.-Z., Wu, H., Wang, Z., Wang, Y., Shen, X.J., Lu, C.H., Quaye-Ballard, J.A., Chen,
632 Y.-H., Zhao, Y.-H., 2017. Monitoring rangeland degradation using a novel local NPP scaling based
633 scheme over the “Three-River Headwaters” region, hinterland of the Qinghai-Tibetan Plateau. *Quat. Int.*
634 444, 97–114. <https://doi.org/10.1016/J.QUAINT.2016.07.050>

635 An, R., Xu, X.F., Yang, R.M., 2014. Time-Lag Effect of Vegetation NDVI on Regional Climate in “Three River
636 Source” Region. *Geomatics Spat. Inf. Technol.* 37, 1–5.

637 Bai, Z.G., Dent, D.L., Olsson, L., Schaepman, M.E., 2008. Proxy global assessment of land degradation. *Soil
638 Use Manag.* 24, 223–234. <https://doi.org/10.1111/j.1475-2743.2008.00169.x>

639 Bastin, G., Scarth, P., Chewings, V., Sparrow, A., Denham, R., Schmidt, M., O’Reagain, P., Shepherd, R.,
640 Abbott, B., 2012. Separating grazing and rainfall effects at regional scale using remote sensing imagery: A
641 dynamic reference-cover method. *Remote Sens. Environ.* 121, 443–457.
642 <https://doi.org/10.1016/j.rse.2012.02.021>

643 Brown de Colstoun, E., Kravitz, L.L., Prince, S.D., 1998. Evidence from rain- use efficiencies does not indicate
644 extensive Sahelian desertification. *Glob. Chang. Biol.* 4, 359–374.
645 <https://doi.org/10.1046/j.1365-2486.1998.00158.>

646 Burrell, A.L., Evans, J.P., Liu, Y., 2017. Detecting dryland degradation using Time Series Segmentation and
647 Residual Trend analysis (TSS-RESTREND). *Remote Sens. Environ.* 197, 43–57.
648 <https://doi.org/10.1016/j.rse.2017.05.018>

649 Cai, H., Yang, X., Xu, X., 2015. Human-induced grassland degradation/restoration in the central Tibetan
650 Plateau: The effects of ecological protection and restoration projects. *Ecol. Eng.* 83, 112–119.
651 <https://doi.org/10.1016/j.ecoleng.2015.06.031>

652 Chen, Q., Zhou, Q., Zhang, H.F., Liu, F.G., 2010. Spatial disparity of NDVI response in vegetation growing
653 season to climate change in the Three-River Headwaters Region. *Ecol. Environ. Sci.* 19, 1284–1289.

654 de Jong, R., de Bruin, S., de Wit, A., Schaepman, M.E., Dent, D.L., 2011. Analysis of monotonic greening and
655 browning trends from global NDVI time-series. *Remote Sens. Environ.* 115, 692–702.
656 <https://doi.org/10.1016/j.rse.2010.10.011>

657 Eddy, I.M.S., Gergel, S.E., Coops, N.C., Henebry, G.M., Levine, J., Zerriffi, H., Shibkov, E., 2017. Integrating
658 remote sensing and local ecological knowledge to monitor rangeland dynamics. *Ecol. Indic.* 82, 106–116.
659 <https://doi.org/10.1016/j.ecolind.2017.06.033>

660 Evans, J., Geerken, R., 2004. Discrimination between climate and human-induced dryland degradation. *J. Arid
661 Environ.* 57, 535–554. [https://doi.org/10.1016/S0140-1963\(03\)00121-6](https://doi.org/10.1016/S0140-1963(03)00121-6)

662 Fensholt, R., Langanke, T., Rasmussen, K., Reenberg, A., Prince, S.D., Tucker, C., Scholes, R.J., Le, Q.B.,
663 Bondeau, A., Eastman, R., Epstein, H., Gaughan, A.E., Hellden, U., Mbow, C., Olsson, L., Paruelo, J.,
664 Schweitzer, C., Seaquist, J., Wessels, K., 2012. Greenness in semi-arid areas across the globe 1981–2007 -
665 an Earth Observing Satellite based analysis of trends and drivers. *Remote Sens. Environ.* 121, 144–158.
666 <https://doi.org/10.1016/j.rse.2012.01.017>

667 Fu, B.P., 1983. Mountain climate. Science Press, Beijing.

668 Gao, J.G., Zhang, Y.L., Liu, L.S., Wang, Z.F., 2014. Climate change as the major driver of alpine grasslands
669 expansion and contraction: A case study in the Mt. Qomolangma (Everest) National Nature Preserve,
670 southern Tibetan Plateau. *Quat. Int.* 336, 108–116. <https://doi.org/10.1016/j.quaint.2013.09.035>

671 Gao, Z.H., Li, Z.Y., Ding, G.D., Li, L.Y., 2005. New approach for desertification assessment by remote sensing
672 based upon Rain Use Efficiency of vegetation. *Sci. Soil Water Conserv.* 3, 37–41.

673 Gardiner, B., Berry, P., Moulia, B., 2016. Review: Wind impacts on plant growth, mechanics and damage. *Plant
674 Sci.* 245, 94–118. <https://doi.org/10.1016/j.plantsci.2016.01.006>

675 Geerken, R., Ilaiwi, M., 2004. Assessment of rangeland degradation and development of a strategy for
676 rehabilitation. *Remote Sens. Environ.* 90, 490–504. <https://doi.org/10.1016/j.rse.2004.01.015>

677 Gu, Z.H., Shi, P.J., Chen, J., 2010. Estimation of grassland degradation based on maximum response of
678 vegetation to climate. *J. Nat. Disasters* 19, 13–20.

679 Harris, R.B., 2010. Rangeland degradation on the Qinghai-Tibetan plateau: A review of the evidence of its
680 magnitude and causes. *J. Arid Environ.* 74, 1–12. <https://doi.org/10.1016/j.jaridenv.2009.06.014>

681 Holben, B.N., 1986. Characteristics of maximum-value composite images from temporal AVHRR data. *Int. J.*
682 *Remote Sens.* 7, 1417–1434.

683 Holm, A.M.R., Cridland, S.W., Roderick, M.L., 2003. The use of time-integrated NOAA NDVI data and
684 rainfall to assess landscape degradation in the arid shrubland of Western Australia. *Remote Sens. Environ.*
685 85, 145–158. [https://doi.org/10.1016/S0034-4257\(02\)00199-2](https://doi.org/10.1016/S0034-4257(02)00199-2)

686 Houerou, L., Henri N., 1984. Rain use-efficiency: a unifying concept in arid-land ecology. *J. Arid Environ.* 7,
687 213–247.

688 Huang, Q.X., Zhao, Y., He, Q., 2013. Climatic Characteristics in Central Asia Based on CRU Data. *Arid Zo.*
689 *Res.* 30, 396–403.

690 J.He, K.Yang, n.d. China Meteorological Forcing Dataset. Cold and Arid Regions Science Data Center at
691 Lanzhou, 2011 [WWW Document]. <https://doi.org/10.3972/westdc.002.2014.db,2014>

692 Karnieli, A., Bayarjargal, Y., Bayasgalan, M., Mandakh, B., Dugarjav, C., Burgheimer, J., Khudulmur, S.,
693 Bazha, S.N., Gunin, P.D., 2013. Do vegetation indices provide a reliable indication of vegetation
694 degradation? A case study in the Mongolian pastures. *Int. J. Remote Sens.* 34, 6243–6262.
695 <https://doi.org/10.1080/01431161.2013.793865>

696 Leroux, L., Bégué, A., Lo Seen, D., Jolivot, A., Kayitakire, F., 2017. Driving forces of recent vegetation
697 changes in the Sahel: Lessons learned from regional and local level analyses. *Remote Sens. Environ.* 191,
698 38–54. <https://doi.org/10.1016/j.rse.2017.01.014>

699 Li, A., Wu, J., Huang, J., 2012. Distinguishing between human-induced and climate-driven vegetation changes:
700 A critical application of RESTREND in inner Mongolia. *Landsc. Ecol.* 27, 969–982.
701 <https://doi.org/10.1007/s10980-012-9751-2>

702 Li, B., 1997. The Rangeland Degradation in North China and Its Preventive Strategy. *Sci. Agric. Sin.* 30, 1–9.

703 Li, C.X., Rogier de Jong, Bernhard Schmid, Hendrik Wulf, Michael E. Schaepman, 2020. Changes in grassland
704 cover and in its spatial heterogeneity indicate degradation on the Qinghai-Tibetan Plateau. *Ecological*
705 *Indicators* 119, 106641, 1–12.

706 Li, L., Li, F.-X., Guo, A.-H., Al., E., 2006. Study on the Climate Change Trend and Its Catastrophe over “The
707 Source Region of Three Rivers” Region in Recent 43 Years. *J. Nat. Resour.* 21, 79–85.

708 Li, N., Zhan, P., Pan, Y., Zhu, X., Li, M., Zhang, D., 2020. Comparison of remote sensing time-series
709 smoothing methods for grassland spring phenology extraction on the Qinghai–Tibetan plateau. *Remote*
710 *Sens.* 12, 1–26. <https://doi.org/10.3390/rs12203383>

711 Liu, J., Xu, X., Shao, Q., 2008. The spatial and temporal characteristics of grassland degradation in the
712 three-river headwaters region in Qinghai Province. *Acta Geogr. Sin.* 63, 364–376.

713 Liu, M.C., Li, D.Q., Luan, X.F., Wen, Y.M., 2005. Ecosystem services and its value evaluation of San Jiang
714 Yuan Region. *J. Plant Resour. Environ.* 14, 40–43.

715 Lu, L., 2011. Study on Grassland Degradation Monitoring in the Source of Three Rivers considering the impact
716 of climate fluctuations. Hohai University.

717 Lu, Z.Y., Cai, F., Liu, W.M., Yuan, Z.P., Chen, Y.Q., Chen, M.Q., 2009. Spatial interpolation methods of wind
718 relative humidity and cloud cover in villages and towns weather forecast in Liaoning province. *J.*
719 *Meteorol. Environ.* 25, 54–57.

720 Meroni, M., Schucknecht, A., Fasbender, D., Rembold, F., Fava, F., Mauclair, M., Goffner, D., Di Lucchio,
721 L.M., Leonardi, U., 2017. Remote sensing monitoring of land restoration interventions in semi-arid
722 environments with a before–after control-impact statistical design. *Int. J. Appl. Earth Obs. Geoinf.* 59, 42–

723 52. <https://doi.org/10.1016/j.jag.2017.02.016>

724 Nicholson, S.E., Tucker, C.J., Ba, M.B., 1998. Desertification, drought, and surface vegetation: An example
725 from the West African Sahel. *Bull. Am. Meteorol. Soc.* 79, 815–829.
726 [https://doi.org/10.1175/1520-0477\(1998\)079<0815:DDASVA>2.0.CO;2](https://doi.org/10.1175/1520-0477(1998)079<0815:DDASVA>2.0.CO;2)

727 Pan, D.F., 2007. Study on the Types and Grades of “Black Soil Type” Degraded Grassland in the Sanjiangyuan
728 Region. Gansu Agricultural University.

729 Prince, S.D., 2012. Mapping Desertification in Southern Africa, in: G.Gutman, A.Janetos, C.O.Justice,
730 E.F.Moran, J.F.Mustard, R.Rindfuss, D.Skole, B.L.Turner (Eds.), *Land Change Science: Observing,
731 Monitoring, and Understanding Trajectories of Change on the Earth’s Surface*. Springer, Berlin, pp. 163–
732 184. https://doi.org/10.1007/978-1-4020-2562-4_10

733 Prince, S.D., Becker-Reshef, I., Rishmawi, K., 2009. Detection and mapping of long-term land degradation
734 using local net production scaling: Application to Zimbabwe. *Remote Sens. Environ.* 113, 1046–1057.
735 <https://doi.org/10.1016/j.rse.2009.01.016>

736 Qian, S., Fu, Y., Pan, F.F., 2010. Climate change tendency and grassland vegetation response during the growth
737 season in Three-River Source Region. *Sci. China Earth Sci.* 53, 1506–1512.
738 <https://doi.org/10.1007/s11430-010-4064-2>

739 Qian, S., Mao, L.X., Zhang, Y.H., 2007. Evaluation models of meteorological conditions for vegetation growth
740 on natural grasslands in China. *Chinese J. Ecol.* 26, 1499–1504.

741 Quaye-Ballardq, J.A., 2014. Drought Impact Assessment on Rangeland Degradation at the Source Region of
742 Yangtze, Yellow and Lancang Rivers. Hohai University.

743 Sandra, E., Fabia, H., Hanspeter, L., Elias, H., 2015. Trend analysis of MODIS NDVI time series for detecting
744 land degradation and regeneration in Mongolia. *J. Arid Environ.* 113, 16–28.

745 Seaquist, J.W., Hickler, T., Eklundh, L., Ardö, J., Heumann, B.W., 2008. Disentangling the effects of climate
746 and people on Sahel vegetation dynamics. *Biogeosciences Discuss.* 5, 3045–3067.
747 <https://doi.org/10.5194/bgd-5-3045-2008>

748 Shen, X., An, R., Feng, L., Ye, N., Zhu, L., Li, M., 2018. Vegetation changes in the Three-River Headwaters
749 Region of the Tibetan Plateau of China. *Ecol. Indic.* 93, 804–812.
750 <https://doi.org/10.1016/j.ecolind.2018.05.065>

751 Stow, D.A., Hope, A., McGuire, D., Verbyla, D., Gamon, J., Huemmrich, F., Houston, S., Racine, C., Sturm,
752 M., Tape, K., Hinzman, L., Yoshikawa, K., Tweedie, C., Noyle, B., Silapaswan, C., Douglas, D., Griffith,
753 B., Jia, G., Epstein, H., Walker, D., Daeschner, S., Petersen, A., Zhou, L., Myneni, R., 2004. Remote
754 sensing of vegetation and land-cover change in Arctic Tundra Ecosystems. *Remote Sens. Environ.* 89,
755 281–308. <https://doi.org/10.1016/j.rse.2003.10.018>

756 Sun, M.Q., 2015. Temporal and spatial pattern of rangeland degradation and its influence factors for the Three
757 River Headwaters Region from 1982 to 2012. Hohai University.

758 Verón, S.R., Paruelo, J.M., Oesterheld, M., 2006. Assessing desertification. *J. Arid Environ.* 66, 751–763.
759 <https://doi.org/10.1016/j.jaridenv.2006.01.021>

760 Vetter, S., 2005. Rangelands at equilibrium and non-equilibrium: Recent developments in the debate. *J. Arid
761 Environ.* 62, 321–341. <https://doi.org/10.1016/j.jaridenv.2004.11.015>

762 Wang, J., Li, W.J., Song, D.M., Tang, H., Dong, G.R., 2004. The analysis of land desertification changing of
763 Minqin County in recent 30 years. *J. Remote Sens.* 8, 282–288.

764 Wang, K., 2004. Grassland restoration and reconstruction. Chemical Industry Press, Beijing.

765 Wang, S.W., Yi, G.H., Gao, Y, P., Zhang, T.B., Bie, X.J., 2014. The research of quantitative relationship
766 between land surface temperature and land cover in Three-River Source Region based on MODIS data.

767 Geomatics Spat. Inf. Technol. 37, 56–61.

768 Wessels, K.J., Prince, S.D., Malherbe, J., Small, J., Frost, P.E., VanZyl, D., 2007. Can human-induced land
769 degradation be distinguished from the effects of rainfall variability? A case study in South Africa. *J. Arid*
770 *Environ.* 68, 271–297. <https://doi.org/10.1016/j.jaridenv.2006.05.015>

771 Wessels, K.J., Prince, S.D., Reshef, I., 2008. Mapping land degradation by comparison of vegetation production
772 to spatially derived estimates of potential production. *J. Arid Environ.* 72, 1940–1949.
773 <https://doi.org/10.1016/j.jaridenv.2008.05.011>

774 Wu, Z., Li, F., Zhang, L., Zhang, J., Du, J., 2014. Research on grassland degradation of Three-river Headwaters
775 Region based on reference vegetation coverage. *J. Nat. Disasters* 23, 94–102.
776 <https://doi.org/10.13577/j.jnd.2014.0213>

777 Xu, D.Y., Kang, X.W., Zhuang, D.F., Pan, J.J., 2010. Multi-scale quantitative assessment of the relative roles of
778 climate change and human activities in desertification - A case study of the Ordos Plateau, China. *J. Arid*
779 *Environ.* 74, 498–507. <https://doi.org/10.1016/j.jaridenv.2009.09.030>

780 Xue, X., Guo, J., Han, B., Sun, Q., Liu, L., 2009. The effect of climate warming and permafrost thaw on
781 desertification in the Qinghai-Tibetan Plateau. *Geomorphology* 108, 182–190.
782 <https://doi.org/10.1016/j.geomorph.2009.01.004>

783 Yan, Y., 2008. Differentiation of related concepts of grassland degradation. *Acta Prataculturae Sin.* 17, 93–99.

784 Yang, R.M., 2012. Research on ecosystem function indicator for vegetation degradation detection in the “Three
785 River Headwaters Region. Hohai University.

786 Yu, H., 2013. Dynamics of Grassland Growth and Its Response to Climate Change on Tibetan Plateau. Lanzhou
787 University.

788 Yu, X.Y., Shao, Q.Q., Liu, J.Y., 2012. Spectral analysis of different degradation level alpine meadows in
789 “Three-river headwaters” region. *Chinese J. Geo-Information Sci.* 14, 398–404.

790 Zhang, Y., Zhang, C. Bin, Wang, Z.Q., Yang, Y., Zhang, Y.Z., Li, J.L., An, R., 2017. Quantitative assessment
791 of relative roles of climate change and human activities on grassland net primary productivity in the
792 Three-River Source Region, China. *Acta Prataculturae Sin.* 26, 1–14.
793 <https://doi.org/10.11686/cyxb2016420>

794 Zhang, Y.X., Fan, J.W., Cao, W., Zhang, H.Y., 2017. Spatial and temporal dynamics of grassland yield and its
795 response to precipitation in the Three River Headwater Region from 2006 to 2013. *Acta Prataculturae Sin.*
796 26, 10–19. <https://doi.org/10.11686/cyxb2017008>

797 Zhao, F., 2012. Temporal and spatial variation and driving factors analysis of vegetation index (MODIS
798 NDVI/EVI) of grasslands in the Three-Rivers Headwaters region. Qinghai University.

799 Zika, M., Erb, K.H., 2009. The global loss of net primary production resulting from human-induced soil
800 degradation in drylands. *Ecol. Econ.* 69, 310–318. <https://doi.org/10.1016/j.ecolecon.2009.06.014>

801